TESTING A MULTI-SENSOR SYSTEM FOR HYDROCEPHALUS MONITORING IN EXTERNAL VENTRICULAR DRAINS

Trevor Hudson[1], Alex Baldwin[1], Eisha Christian[2], J. Gordon McComb[2,3], and Ellis Meng[1]
[1]Department of Biomedical Engineering, University of Southern California, USA
[2]Keck School of Medicine, University of Southern California, USA
[3]Division of Neurosurgery, Children's Hospital Los Angeles, USA

ABSTRACT

We report a multi-sensor system for monitoring cerebrospinal fluid (CSF) dynamics in hydrocephalus shunts. Flow and biofouling sensors based on electrochemical impedance transduction were integrated into a single thin film die designed to be packaged in-line for compatibility with existing clinical workflows. Custom electronics provided remote impedance measurement, analysis, and data storage. This multi-sensor system was designed for use in external ventricular drains (EVDs), which drain CSF from the brain's ventricles to reduce acute swelling and manage intracranial pressure. The direct fluidic connection via an implanted catheter to the ventricles is similar to that of implanted hydrocephalus shunts, making EVDs a suitable model for preliminary non-invasive sensor validation. The multi-sensor system was validated on the benchtop in an EVD model using both saline and CSF collected from human patients. Flow resolution was 48.8 µL/min within a range of -330 to 660 µL/min (average CSF flow: 50 to 317 µL/min [1]). Successful benchtop validation will inform upcoming clinical tests in patients with EVDs.

INTRODUCTION

Hydrocephalus is characterized by a pathological buildup of CSF in the brain. If left untreated, increased intracranial pressure (ICP) results in cranial swelling and compression of brain tissue, leading to severe neurological symptoms and eventually death. Congenital hydrocephalus occurs in 1 to 2 of every 1000 births [2] and continues to afflict patients throughout their lives. Hydrocephalus is typically treated via lifelong implantation of a silicone shunt to drain excess fluid into the abdomen. Unfortunately, this intervention suffers a high failure rate, with some 30-40% of shunts failing by year 1 and 60-70% by year 3 [3]; over half of these failures are due to catheter occlusion [4]. Early stages of shunt failure lead to nonspecific symptoms, such as headache and vomiting; diagnosing failure requires multiple imaging studies and invasive tests [5]. A sensorized shunt could transmit vital information about CSF flow and shunt function, eliminating the need for scans and improving patient outcomes and quality of life [6].

Intra-shunt flow transducers have been reported which utilize a pressure differential and Bernoulli's principle [7] or a heater and resistance temperature detector (RTD) [8], [9]. We previously developed thin-film polymer flow sensors based on the impedance between exposed electrodes, which is highly sensitive to heat flow from a microfabricated heater placed upstream [10], [11]. By measuring impedance of fluid directly, these sensors outperform traditional thermal flow sensors, which utilize RTDs to detect heat flow and require hermetic encapsulation *in vivo*.

Biofouling is the accumulation of unwanted biological matter on surfaces. Proteins such as albumin and fibrinogen absorb to polymer surfaces just seconds after contact [12] and can stimulate the adhesion and proliferation of astrocytic tissue ingrowth, leading to shunt occlusion and instigating further damaging immune responses [13]. Progenitors of tissue encapsulation like fibroblasts and glial cells also proliferate on platinum [14], which can degrade signal quality of implanted sensors. Bacterial or fungal growth on shunt hardware also affects 3-20% of implanted shunts, and is one of the most urgent complications which typically requires full shunt replacement [15]. Label-free, rapid detection of biofouling is an area of ongoing research [16]; recently, Kim et al. demonstrated that impedance spectroscopy between exposed electrodes can monitor biofouling [17].

An acute intervention for elevated ICP is the EVD, in which the shunt is passed percutaneously to drain CSF into a bag. EVDs are typically placed for about 2 weeks [18] in response to traumatic brain injury or hemorrhage.

Here, we demonstrate a polymer multi-sensor module targeting flow and biofouling, and a portable electronic system which autonomously operates each sensor. Prior to *in vivo* demonstration in animal or human, sensors were fabricated and evaluated using a benchtop EVD model which presents a strategic test platform for hydrocephalus without requiring implantation. Sensors were designed and packaged for in-line placement in the EVD flow path, exposing them to human CSF under realistic pressure and flow conditions.

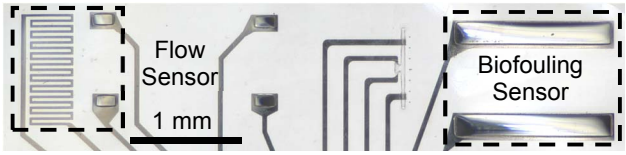

Figure 1: The multi-sensor system combines impedimetric flow and biofouling sensors on a single die. Additional features are test structures. All sensors operate using electrochemical impedance measurement through CSF and do not require hermetic encapsulation.

DEVICE DESIGN AND FABRICATION

Polymer Multi-sensor Device

Flow and biofouling sensors were fabricated on a single sensor die using biocompatible materials: platinum for electrical and electrochemical elements and Parylene C as the substrate (Figure 1). As described elsewhere [10], the flow sensors consists of a resistive heater and downstream temperature sensor. As flow rate increases, heat transfer via

forced convection proceeds at a faster rate toward the temperature sensor, changing the profile of the resultant temperature versus time curve. Temperature sensing is achieved via measurement of electrochemical impedance between two exposed electrodes. At sufficiently high frequencies, the double-layer capacitance, which naturally forms at the electrode-electrolyte interface to measure solution resistance, is bypassed. The solution resistance possesses a significantly higher temperature coefficient of resistance compared to RTDs and is used for sensing.

The biofouling sensor operates via recording of the impedance spectrum between two exposed electrodes. The surface area of these electrodes is large, as opposed to non-sensing regions of the device, to maximize the exposure and adherence of biofouling particles or cells . We expect impedance magnitude and phase to increase as the sensor surface becomes increasing obscured.

Sensor fabrication follows previously reported methods [19], [20] in which two 15 µm thick layers of Parylene C sandwich a 2000 Å thick layer of patterned platinum. The flow sensor's heater is a serpentine trace with 25 µm pitch and spacing and nominal resistance of 400 Ω. Temperature sensing electrodes measured 80×180 µm, were placed 500 µm downstream of the heater, and were spaced 700 µm apart. These parameters were chosen based on results from our prior work [10]. The biofouling sensors measured 200×1500 µm with 860 µm spacing and were previously used to monitor shunt patency [21].

Electronic Measurement System

A custom electronic datalogger board was designed for automated impedance measurement in the clinic (Figure 2). An AD5933 network analyzer provided a buffered input to a multiplexing chip, which routed signals between the flow and biofouling sensors. After passing through the polymer device, the return signal was amplified with a current-to-voltage topology and passed back to the network analyzer for impedance calculations. A Teensy 3.2 microcontroller handled all I/O and timing operations. Data was stored on a local microSD card. Electrochemical impedance spectroscopy (EIS) data was acquired between 1 to 100 kHz using the full range of the network analyzer; flow measurements were taken at 50 kHz, where phase of the full system was minimized. EIS was acquired at 2 samples per second to minimize power draw, but measurement at a rate of 20 Hz is possible. The datalogger was deactivated to a quiescent mode when not in use.

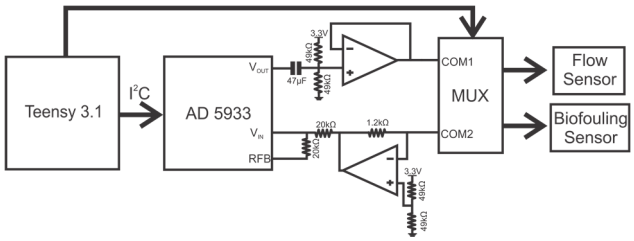

Figure 2: The data collection platform used an AD5933 network analyzer chip to measure electrochemical impedance across sensor electrodes.

Packaging and System Design

External electrical contact with the polymer device was achieved by addition of a thin polyetheretherketone spacer to support the contact pads, then insertion of the assembly into a zero insertion force connector. Devices were then inserted into the lumen of a luer lock module (ID 3.25 mm) via a milled slit to enable simple connection to clinical EVDs (Figure 3). The inline sensor is positioned centrally in the lumen to detect maximum fluid velocity in the laminar stream (Re = ~1.30).

Though our system is amenable to wireless operation, a wired system was pursued to limit complexity and maximize clinical data yield. A 0.5-meter 12 pin cable connected the datalogger and polymer device. A 2000 mAh lithium ion battery allowed for 3-4 days of continuous measurement.

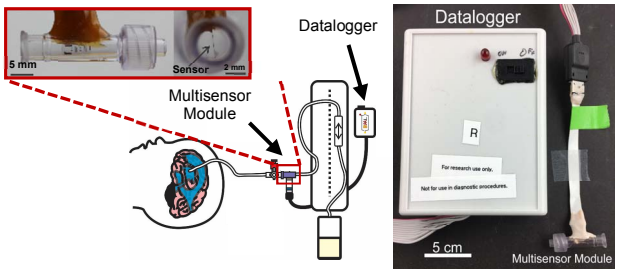

Figure 3: The system consists of a multi-sensor module embedded in a luer lock spacer (inset), which is placed in-line with an EVD's drain and attached to a custom data collection and analysis platform. The system's portability, long lifetime, and simple packaging (right) enables simple integration into clinical workflows.

EXPERIMENTAL METHODS

All measurements were obtained using the portable measurement system described. Short term flow sensing performance was characterized using 1x phosphate buffered saline (PBS) flow set by a calibrated syringe pump. Longer term tests were conducted on a benchtop EVD model consisting of a Sophysa RE-1031 proximal catheter sealed in a vial filled with deidentified human CSF which was maintained at 37° C on a hot plate. A peristaltic pump simulated physiological pulsatile flow, which naturally occurs *in vivo* due to respiratory and cardiac waves [22]. Accuracy was references against measurements from a Sensirion SLI-1000 flowmeter.

Acquiring one flow reading entails three measurement steps (Figure 4a). Impedance is first measured with the heater off to acquire a baseline. The heater is then activated and a heating curve is measured. Afterwards, a pause between measurements is taken to allow the sensor to cool. Each timespan can be tuned to trade sensor performance for time resolution; here, we used 10 seconds for each period for simplicity. Three such measurements were acquired and averaged for each data point to measure and mitigate sensor variance.

RESULTS AND DISCUSSION

Initial benchtop characterization demonstrated a low noise of <0.1% of the measured baseline impedances, indicating viability of the system for precise and repeatable

flow measurements (Figure 4b). We generated several heat curves sequentially to further test repeatability, observing an average standard deviation of only 12.3 Ω across all 60 measurements.

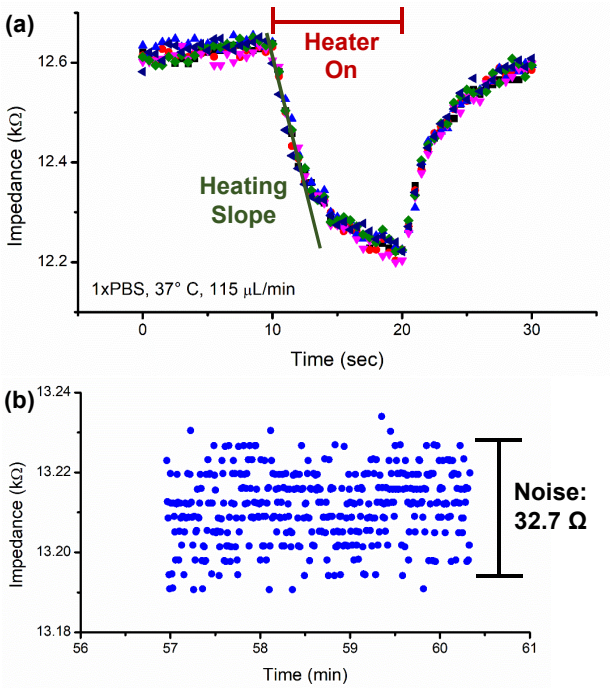

Figure 4: (a) Noise levels were low enough (32.7 Ω) for accurate measurement of impedance changes <0.1%, which is necessary for flow sensor operation. (b) The impedance electronics could repeatably resolve slight impedance changes necessary for flow sensor operation. Representative data is shown for six trials using the same device.

The profile of the impedance versus time curve depends on flow rate. A variety of quantities can be extracted from this curve to transduce flow. We chose to use the minimum rate of change of impedance with time after evaluating this method against other quantities (results not shown). This method transduced flow rate at a 48.8 µL/min resolution (2σ).

Flow sensor performance was compared between PBS and CSF at room and body temperature (Figure 5). A temperature effect was present at negative and low positive flow rates, indicating future calibrations must be recorded at body temperature. However, PBS and CSF data were statistically identical ($p>0.1$) except for ±165µL/min at 37°C, which is attributed to noise in our setup.

Flow was measured hourly for 44 hours in human CSF in our benchtop EVD model (Figure 6). RMS error against a reference flow sensor was 40.6 µL/min. At 42 hours, we clearly detect the drop in flow caused by a simulated shunt occlusion. We observed that absolute error began to increase exponentially after about 24 hours. We suspect this was due to changes in ionic concentration of the CSF associated with evaporation, although solution volume or conductivity data was not available to confirm this.

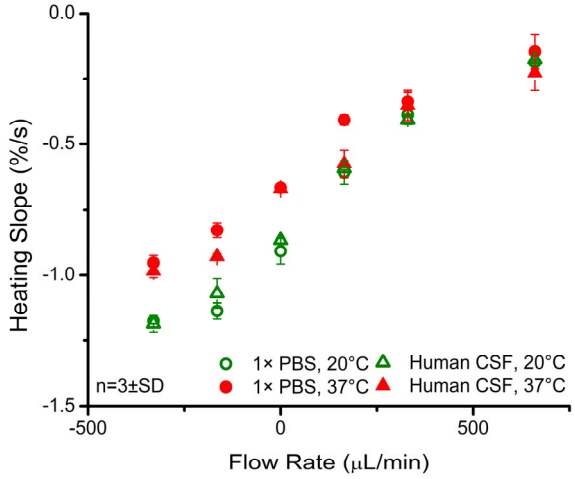

Figure 5: The flow sensor was calibrated in both 1× PBS and human CSF, at room and body temperatures, using the "heating slope" method. A marked temperature effect exists at negative and low positive flow rates.

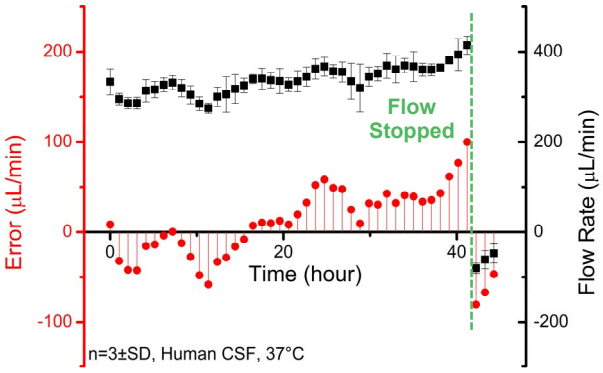

Figure 6: A 44-hour flow test using human CSF was conducted using our benchtop EVD model. We successfully detected the zero-flow condition at 42 hours.

We evaluated our biofouling sensor by coating in cyanoacrylate to simulate biological particle adhesion (Figure 7). Progressively larger changes in impedance phase occurred with sensor occlusion. Additional testing was performed by immersion in flowing human cerebrospinal fluid at body temperature for 12 days to capture the full duration of most EVD placements [23] (Figure 8). No change in phase was observed, suggesting sufficient biofouling to impact sensor operation does not occur during operation.

CONCLUSION

In this paper, a system for the monitoring of CSF in implanted shunts was discussed, consisting of a thin-film polymer device containing flow and biofouling sensors, and a portable, autonomous printed circuit for data collection, analysis, and storage. Sensors were validated with a benchtop EVD model in PBS and human CSF. Future work will involve validating the flow sensor over longer timespans, integrating temperature sensing, and investigating alternate biofouling sensor geometries.

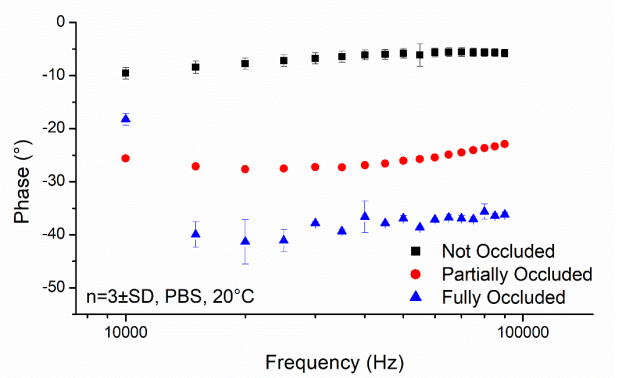

Figure 7: A decrease in phase was detected across the impedance spectrum after coating in cyanoacrylate to simulate biofouling.

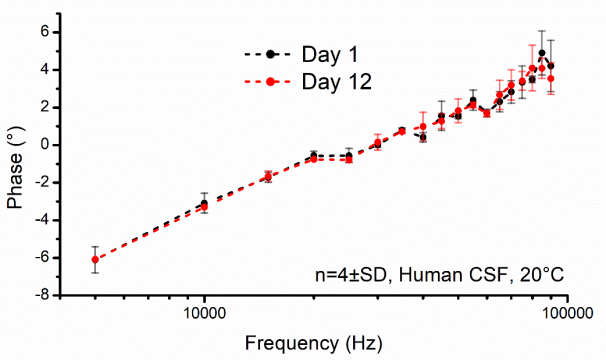

Figure 8: The biofouling sensor was tested on the benchtop using CSF collected from patients at a local hospital; no significant shift in EIS between patency electrodes (indicative of electrode degradation or biofouling) occurred after 12 days.

REFERENCES

[1] J. M. Drake *et al.*, "Cerebrospinal Fluid Flow Dynamics in Children with External Ventricular Drains," *Neurosurgery*, vol. 28, no. 2, pp. 242–250, Feb. 1991.

[2] "Hydrocephalus Fact Sheet | National Institute of Neurological Disorders and Stroke."

[3] J. M. Drake *et al.*, "Randomized Trial of Cerebrospinal Fluid Shunt Valve Design in Pediatric Hydrocephalus," *Neurosurgery*, vol. 43, no. 2, pp. 294–303, Aug. 1998.

[4] J. J. Stone *et al.*, "Revision rate of pediatric ventriculoperitoneal shunts after 15 years," *Journal of Neurosurgery: Pediatrics*, vol. 11, no. 1, pp. 15–19, 2013.

[5] A. A. Khan *et al.*, "Cerebrospinal shunt malfunction: recognition and emergency management," *British Journal of Hospital Medicine*, vol. 68, no. 12, pp. 651–655, Dec. 2007.

[6] B. R. Lutz *et al.*, "New and improved ways to treat hydrocephalus: Pursuit of a smart shunt," *Surg Neurol Int*, vol. 4, no. Suppl 1, pp. S38–S50, 2013.

[7] A. Narayanaswamy, "A wireless monitoring system for Hydrocephalus shunts," IEEE EMBC, 2015.

[8] T. Bork *et al.*, "Development and in-vitro characterization of an implantable flow sensing transducer for hydrocephalus," *Biomed Microdevices*, vol. 12, no. 4, pp. 607–618, 2010.

[9] C. Li *et al.*, "Smart catheter flow sensor for continuous regional cerebral blood flow monitoring," in *2011 IEEE SENSORS*, 2011, pp. 1417–1420.

[10] A. Baldwin *et al.*, "An Electrochemical Impedance-Based Thermal Flow Sensor for Physiological Fluids," *Journal of Microelectromechanical Systems*, vol. 25, no. 6, pp. 1015–1024, Dec. 2016.

[11] A. Baldwin *et al.*, "A calorimetric flow sensor for ultra-low flow applications using electrochemical impedance," in *2018 IEEE Micro Electro Mechanical Systems (MEMS)*, 2018, pp. 361–364.

[12] C. N. Cottonaro *et al.*, "Quantitation and Characterization of Competitive Protein Binding to Polymers," *ASAIO Journal*, vol. 27, no. 1, p. 391, 1981.

[13] M. Del Bigio *et al.*, "Biological Reactions to Cerebrospinal Fluid Shunt Devices: A Review of the Cellular Pathology," *Neurosurgery*, vol. 42, no. 2, pp. 319–326, Feb. 1998.

[14] C. P. Pennisi *et al.*, "Responses of fibroblasts and glial cells to nanostructured platinum surfaces," *Nanotechnology*, vol. 20, no. 38, p. 385103, 2009.

[15] J. Prusseit *et al.*, "Epidemiology, Prevention and Management of Ventriculoperitoneal Shunt Infections in Children," *Pediatric Neurosurgery*, vol. 45, no. 5, pp. 325–336, 2009.

[16] L. Yang *et al.*, "Detection of viable Salmonella using microelectrode-based capacitance measurement coupled with immunomagnetic separation," *Journal of Microbiological Methods*, vol. 64, no. 1, pp. 9–16, Jan. 2006.

[17] S. Kim *et al.*, "Rapid bacterial detection with an interdigitated array electrode by electrochemical impedance spectroscopy," *Electrochimica Acta*, vol. 82, pp. 126–131, Nov. 2012.

[18] P. Lackner *et al.*, "Efficacy of Silver Nanoparticles-Impregnated External Ventricular Drain Catheters in Patients with Acute Occlusive Hydrocephalus," *Neurocrit Care*, vol. 8, no. 3, pp. 360–365, 2008.

[19] B. J. Kim *et al.*, "Micromachining of Parylene C for bioMEMS," *Polymers for Advanced Technologies*, vol. 27, no. 5, pp. 564–576, 2016.

[20] C. A. Gutierrez *et al.*, "Epoxy-less packaging methods for electrical contact to parylene-based flat flexible cables," in *2011 16th International Solid-State Sensors, Actuators and Microsystems Conference*, 2011, pp. 2299–2302.

[21] B. J. Kim *et al.*, "Parylene MEMS patency sensor for assessment of hydrocephalus shunt obstruction," *Biomed Microdevices*, vol. 18, no. 5, p. 87, 2016.

[22] S. Holm *et al.*, "The frequency domain versus time domain methods for processing of intracranial pressure (ICP) signals," *Medical Engineering & Physics*, vol. 30, no. 2, pp. 164–170, Mar. 2008.

[23] A. R. Kirmani *et al.*, "Role of external ventricular drainage in the management of intraventricular hemorrhage; its complications and management," *Surg Neurol Int*, vol. 6, Dec. 2015.

CONTACT

*E. Meng, tel: +1-213-740-6952; ellis.meng@usc.edu